inter.noise
HAMBURG 2016

Study of a low-cost end-fire array for use in electric vehicles

Jesús CARBAJO[1]; Stephen ELLIOTT[2]; Jordan CHEER[2]

[1] Department of Physics, Systems Engineering and Signal Theory, University of Alicante, Spain

[2] Institute of Sound and Vibration Research, University of Southampton, United Kingdom

ABSTRACT

Electric Vehicles (EVs) are expected to be equipped with Acoustic Vehicle Alerting System (AVAS) that effectively allow vulnerable pedestrians to detect from which direction EVs are approaching. In this context, directional sound sources have been proposed to provide an effective warning sound where necessary, without being excessively loud in other directions and thus increasing noise pollution. This work explores the use of a low-cost end-fire array as an AVAS in EVs. For this purpose, a numerical model of the array based on transmission line theory was implemented and the acoustic performance of the array was assessed. A parametric study was found very useful to investigate the influence of the array's geometrical parameters on the system response and in understanding the behaviour of the acoustic radiator. Additionally, the well-established equivalent circuit theory was used to propose an analytical model of the array, which was validated against the numerical model with good agreement.

Keywords: Electric vehicles, Warning sounds, Directional sound sources

I-INCE Classification of Subjects Number(s): 11.9.9

1. INTRODUCTION

Electric Vehicles (EVs) are becoming an environmentally friendly alternative to traditional Internal Combustion Engine (ICE) vehicles in terms of lowering CO2 emission and reducing noise pollution in urban areas (1-4). Nevertheless, concerning Noise, Vibration and Harshness (NVH), their "low-noise" behaviour when operating at very low speeds poses a danger to road safety especially in the case of children, elderly, two-wheelers and visually impaired pedestrians (5). For this reason, public authorities are working on legislation (6, 7) to regulate the minimum sound levels required so as to make EVs more easily detectable over background noises. In this context, transport industry professionals together with the scientific community are joining efforts in the development of Acoustic Vehicle Alerting Systems (AVAS) that reduce the hazard to these collectives.

AVAS are warning sound systems to be installed in EVs and intended mainly to make vulnerable pedestrians aware of the vehicle's presence by providing an audible signal (8). Some of the AVAS take advantage of the vehicle's own horn, include a speaker under the hood, or use miniature audio speakers placed on the wheel wells that emit specific sounds as the EV moves. However, the use of these devices has raised some controversy as to increased noise pollution when radiating high noise levels in unwanted directions (9). In this regard, it is desirable to design AVAS that effectively allow pedestrians to detect from which direction EVs are approaching without producing excessive sound levels for others outside the vehicle (10). Hence, the source should not be hidden in the car body and ought to be able to radiate freely only in the moving direction (11). For this purpose, many systems use directional sound equipment that involves the utilization of external speakers, wired or wireless, frequently mounted at the front and rear of the vehicle (embedded in the bumper), allowing the vehicle to be heard by those in its path. The directivity control is usually achieved by using transducer arrays together with electronic filters in what is known as beamformers. Cheer et al. (12) compared two types of these beamformers, broad-side arrays and end-fire arrays, showing that the latter provide higher

[1] jesus.carbajo@ua.es
[2] {s.j.elliott, j.cheer}@soton.ac.uk

directivity than the former. Further, typically studied beamformers can be expensive, so proposing cheaper alternatives contributes to the settlement of such systems. For these reasons, this work explores the use of a low-cost end-fire array (13) as a directional sound source for EVs. Even though the detectability of the EVs will depend strongly on the warning sound features (14), the directivity pattern and acoustic efficiency of the sound sources must also be evaluated. Unfortunately, little work has been done regarding the directional characteristics of AVAS.

This work aimed to develop a model of a low-cost end-fire acoustic radiator with which Electric Vehicles (EVs) are intended to be equipped. Given that the production of Acoustic Vehicle Alerting Systems (AVAS) that meet the needs of road safety required for these vehicles is still a challenge to the EVs industry, proposing new solutions is of great interest. The modeling of the low-cost array allows the potential acoustic behaviour of this system to be predicted and its suitability for the EV application to be assessed. The numerical model implemented is based on transmission line theory, and served to analyze and evaluate the effect of modifying the array's geometrical parameters on its directivity pattern and acoustic efficiency. The adopted methodology leads to a better understanding of these systems and can be used to facilitate their design and analysis. Additionally, an analytical approach that relies on the equivalent circuit theory was used to propose an analytical model of the array, which was validated against the numerical model with good agreement.

The structure of the paper is as follows: in Section 2, the low-cost end-fire array and the numerical model proposed by Holland and Fahy (13) to study its acoustic behaviour are recalled. An analytical approach is then developed to describe the sound propagation throughout the array, and the acoustic indicators used to assess its acoustic performance defined. In Section 3, a case of study is analyzed and the influence of the array's geometrical parameters on the system response investigated by means of a parametric study. The proposed analytical approach is validated against the numerical model. The limits of both models are also discussed. The main conclusions are summarized in Section 4.

2. BACKGROUND THEORY

2.1 Low-cost end-fire arrays

Low-cost end-fire arrays are directive acoustic sources that allow a directional response to be achieved over a certain frequency range. A typically studied configuration consists of a cylindrical pipe with a compression driver attached to one end and periodically arranged circular holes along its axis which act as radiating sources. A foam wedge at the other end of the pipe is used to minimize reflected waves at this end by providing an anechoic termination. The directional response of the array is facilitated by the time delay between the sound radiated from the individual holes, which is introduced by the propagation of the acoustic wave along the length of the pipe. The sound radiated from the holes then interacts to produce a directional response. The working frequency range is dictated largely by the geometrical characteristics of the array (hole radius, a, pipe diameter, d, hole spacing, l, number of holes, n, and pipe thickness, t). Figure 1 shows a diagram of this type of array.

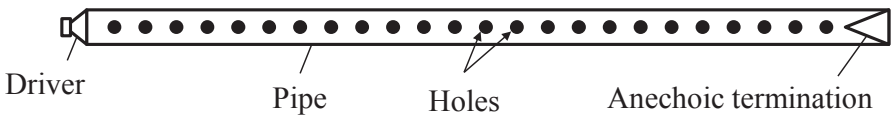

Figure 1 – Diagram of a low-cost end-fire array.

Unlike other more expensive array technologies, it differentiates between the front and rear of the array so that it focuses sound only in the frontal direction, significantly reducing the rear lobe radiation. Another advantage is that it exhibits a good directivity control in the low frequency range without the need for a large array. Furthermore, the overall cost is significantly lower as it uses a single driver and does not require any additional directivity control electronic system. On the other hand, and as it will be demonstrated later, the main drawback of these systems is the trade-off between directivity and acoustic efficiency.

2.2 Numerical model

Holland and Fahy (13) proposed a numerical model that uses transmission line theory to assess the acoustic behaviour of low-cost end-fire arrays whose dimensions are small compared to the wavelength of the sound wave of interest. Further, it is based on the assumptions of plane wave

propagation, no interaction effect between holes and neglecting of viscothermal dissipative effects.

Let us consider the configuration schematically represented in Figure 2.

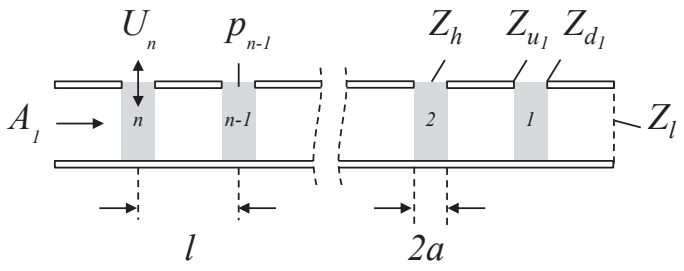

Figure 2 – Schematic diagram of the transmission line model of a low-cost end-fire array.

The total pressure field p_T radiated by the array can be determined from the combination of the effects of n discrete sources positioned along this from (15)

$$p_T = \frac{j\rho_0 c_0 k}{4\pi} \sum_{i=1}^{n} \frac{U_i e^{-jkr_i}}{r_i} \tag{1}$$

where ρ_0 is the air density, c_0 the sound propagation velocity in air, $k = \omega/c_0$ the wave number, ω being the angular frequency, and U_i the volume velocity through each hole source separated a distance r_i from the evaluation point.

These volume velocities can be determined from the acoustic pressure p_i in the region of each hole and its radiation impedance Z_h using the relation

$$U_i = \frac{p_i}{Z_h} \tag{2}$$

The pressure values can be expressed in terms of the "upstream" Z_{ui} and "downstream" Z_{di} acoustic impedances of each hole as

$$p_i = \begin{cases} p_{i+1} \left\{ \dfrac{Z_{u_i}\left(Z_0 + Z_{d_{i+1}}\right)\left(\cos(kl) - j\sin(kl)\right)}{Z_{d_{i+1}}\left(Z_0 + Z_{u_i}\right)} \right\} & i < n \\ 2A_1 \left\{ \dfrac{Z_{u_n}}{Z_{u_n} + Z_0} \right\} & i = n \end{cases} \tag{3}$$

where $Z_0 = \rho_0 c_0 / S$, being S the cross-sectional area of the pipe, and A_1 the amplitude of the incident pressure wave propagating from the driver and impinging on hole n.

The "upstream" and "downstream" acoustic impedances of each hole can be obtained from circuit analysis theory and transmission line basic equations, respectively

$$Z_{u_i} = \frac{1}{1/Z_{d_i} + 1/Z_h} \tag{4}$$

$$Z_{d_i} = Z_0 \left\{ \frac{Z_{u_{i-1}} + jZ_0 \tan(kl)}{Z_0 + jZ_{u_{i-1}} \tan(kl)} \right\} \tag{5}$$

with $Z_{u0} = Z_l = Z_0$, being Z_l the anechoic termination impedance.

Although several representations of the radiation impedance of a hole exist (mainly differing on the end correction terms), the selected one approximates it as if it were a piston in an infinite baffle (assuming the hole size small compared to the pipe diameter). The resulting expression reads

$$Z_h = \rho_0 c_0 \left\{ \frac{k^2}{4\pi} + j \frac{k\left(t+1.5a\right)}{\pi a^2} \right\} \tag{6}$$

this equation being valid for $ka << 1$.

The main advantage of the numerical model is that it is generic and can handle low-cost end-fire array systems of arbitrary geometry, allowing investigations into the effects of the geometry on the directional source behaviour and ultimately its optimization.

2.3 Analytical model

A simplified model of a low-cost end-fire array based on the equivalent circuit theory was developed. This method was very useful to analyse the acoustic wave propagation throughout the array without the need of the numerical model, in addition to shorten the solution time and of their ease to determine physical quantities of interest (e.g. propagation constant).

As a first step, from inspection of the schematic diagram shown in Figure 2, the impedance-type analogous circuit of Figure 3 and its specific lumped elements can be drawn.

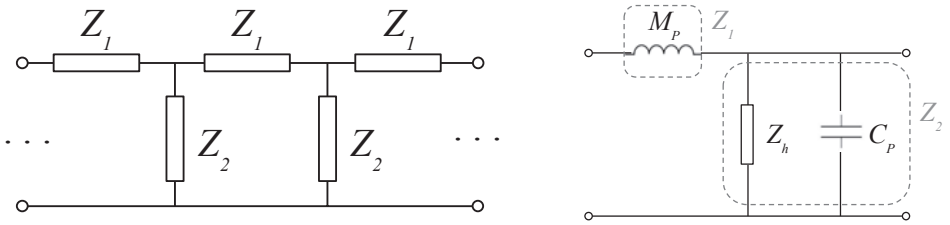

Figure 3 – Schematic diagram of the transmission line model of a low-cost end-fire array.

This equivalent circuit represents a series of two-port elementary components, each representing a section for each hole of the array, and can be used to properly describe the acoustic radiator as a periodic system in the low-frequency (array dimensions small compared to the minimum wavelength of interest). The series inductor $M_p = \rho_0 l/S$ represents the acoustic mass of a pipe section, the shunt capacitor $C_p = lS/(\rho_0 c_0^2)$ its acoustic compliance and Z_h the corresponding hole radiation impedance. The radiation impedance is this time represented by the even simpler resistance-mass shunt analogous circuit of one side plane circular piston in an infinite baffle given in (16), wherein the resistive term is no longer frequency dependent. The shunt radiation resistance R_h and radiation mass M_h of the hole now become

$$R_h = \frac{128\rho_0 c_0}{9\pi^3 a^2} \tag{7}$$

$$M_h = \frac{8\rho_0}{3\pi^2 a} \tag{8}$$

From a single section of the above lumped component model, a simplified description of the acoustic radiator as a periodic system can be derived. The acoustic behaviour of this device can then be described by two well-known parameters, namely characteristic impedance, Z_c, and propagation constant, γ, which are defined as follows

$$Z_c = \sqrt{Z_1 Z_2} \tag{9}$$

$$\gamma = \frac{1}{l}\sqrt{\frac{Z_1}{Z_2}} \tag{10}$$

The parameters derived can be used, for instance, to compare the characteristics of different array designs in a straightforward manner. By inspection of the circuit of Fig. 3, recalling the equation for the propagation constant Eq. (10) and substituting the respective circuit elements, is possible to derive an expression for the cut-off frequency f_0 of the array system such that

$$f_0 = \frac{c_0}{2\pi}\sqrt{\frac{\pi a^2}{lSl_h}} \tag{11}$$

where l_h denotes the hole length (approximated as $l_h \approx 0.85a$ for $ka < 0.5$).

2.4 Acoustic indicators

Since this research mostly focuses on directivity of warning sound systems, the array behaviour was evaluated by means of the directivity index and the acoustic efficiency. The directivity factor Q was chosen to assess the directivity of the array, as it gives the degree of directivity in a single value for each frequency. It can be determined from the total pressure field at a number of points with angles θ_i in a horizontal plane around the array so that

$$Q = \frac{2\left|p_T\left(0^\circ\right)\right|^2}{\sum_{\theta_i=0^\circ}^{180^\circ}\left|p_T\left(\theta_i\right)\right|^2 \sin\left(\theta_i\right)\Delta\theta} \tag{12}$$

where $\Delta\theta$ is the separation in radians of the successive points around the array at which p_T calculations are made. When this number is expressed in decibels it turns to be the directivity index $DI = 10\log_{10}Q$.

Regarding the acoustic efficiency E_{ff}, defining it as the ratio of the acoustic power radiated by the array, W_o, to the acoustic power supplied by the driver, W_i, will yield

$$E_{ff} = \frac{W_o}{W_i} \tag{13}$$

where $W_o = W_i - W_d$, being $W_d = |p_1|^2/Z_0$ the acoustic power dissipated in the anechoic termination and $W_i = |p_n|^2/Re\{Z_{un}\}$.

Additionally, both approaches let us analyse the acoustic wave propagation phenomena inside the pipe for the clear understanding of the underlying physics. This can be achieved by calculating the propagation constant $\gamma = \alpha + j\beta$, which measures the attenuation α and phase shift β undergone by this wave as it propagates through the pipe between different holes. Thus,

$$p_{i-1} = p_i e^{-\gamma l} \tag{14}$$

In the case of the numerical model, the propagation constant of the array is determined by averaging the resulting values from substitution in Eq. (14) of the pressure values calculated in Eq. (3) (it should be noted that only the holes away from the ends of the array should be considered for the calculations). This parameter also offers valuable information on the frequency range at which the array becomes directive effectively and will serve to validate the proposed analytical model.

3. RESULTS

3.1 Case of study

First, the sound radiation of a uniform low-cost end-fire array design was analyzed using the numerical model proposed by Holland and Fahy (13). It was evaluated at a distance of 3.5 m from the center of the array and in the frequency range from 500 to 5000 Hz, where the warning sounds are defined for better detectability (14). The geometrical characteristics chosen for the calculations were: $a = 6$ mm, $d = 40$ mm, $l = 25$ mm, $n = 25$ and $t = 3$ mm; thus being the diameter of the pipe small enough to ensure plane wave propagation along it in the working frequency range and to avoid excitation of transversal modes. Figure 4 shows the Sound Pressure Level (SPL) frequency response as a function of the observation angle for this reference design.

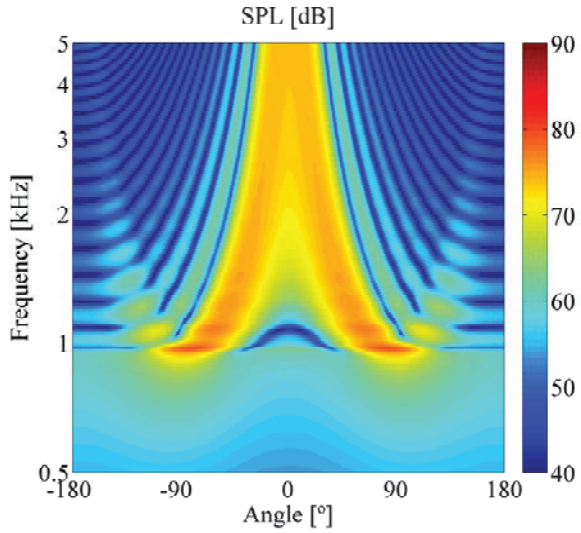

Figure 4 – Sound Pressure Level (SPL) frequency response as a function of the observation angle calculated at a distance of 3.5 m for the reference array design.

It is confirmed the major amplitude of radiation of the low-cost end-fire array in the direction where the main lobe is to be steered. In short, as the frequency increases, the on-axis main lobe becomes more pronounced and the array radiation turns more directional. This feature is beneficial in the application to EVs. It is interesting now to investigate how the geometrical parameters of the array influence its acoustic behaviour, and how their modification can help one to control the directivity. Specifically, the next subsection examines the effect of modifying the hole size and the spacing of the holes.

3.2 Influence of the geometrical parameters

In order to analyse and evaluate the effect of modifying the array geometrical parameters on its directivity index and acoustic efficiency, a parametric numerical study was conducted. By examining the Eqs. (1) to (6), it can be shown that the array performance will depend mainly on the size and spacing of the holes. For this reason, each of these two design parameters was varied while holding the other parameters constant.

3.2.1 Influence of the hole size

Figure 5 shows the effect of varying the hole radius on the directivity index while all remaining parameters are held constant. Fig. 5(a) is a contour map of this parameter with respect to frequency and hole radius, whilst Fig. 5(b) shows directivity index curves for three distinct hole radius extracted from the contour map. Notice that increasing the hole radius forces the lower cut-off frequency (frequency above which the array becomes directional) higher in frequency, worsening the directivity control in the low frequency region.

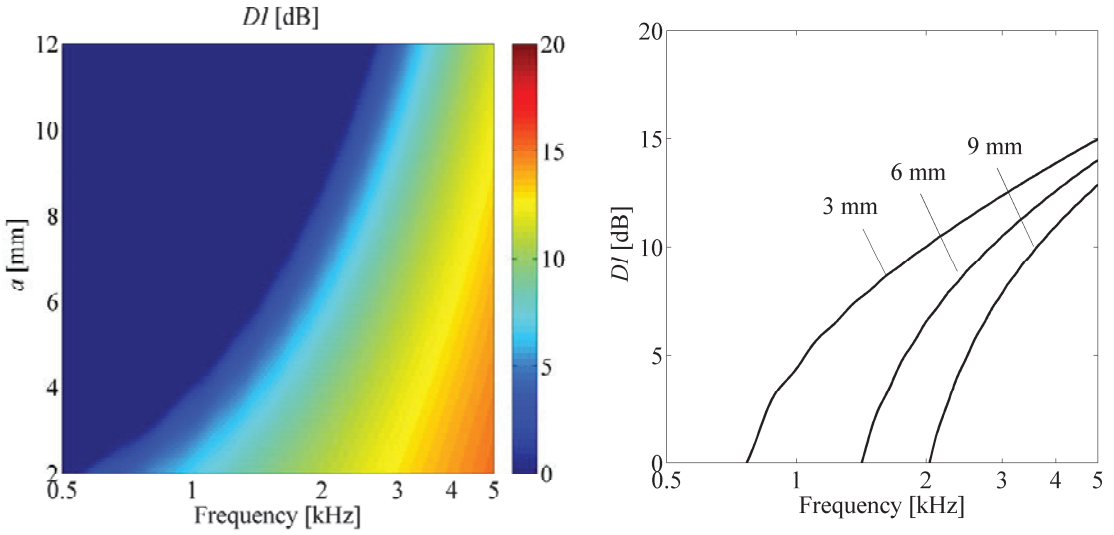

Figure 5 – Effect of the hole radius on the directivity index. (Left) Contour map and (Right) directivity index curves for several radiuses.

Figure 6 presents the acoustic efficiency expressed in decibels for the same configuration with the same variation. Larger holes increase the volume velocity produced at each hole, which in turn broadens the working frequency range in which the acoustic efficiency is high. The ripples in the mid-high frequency region are attributed to the resonances between holes resulting from the impedance mismatch at each hole

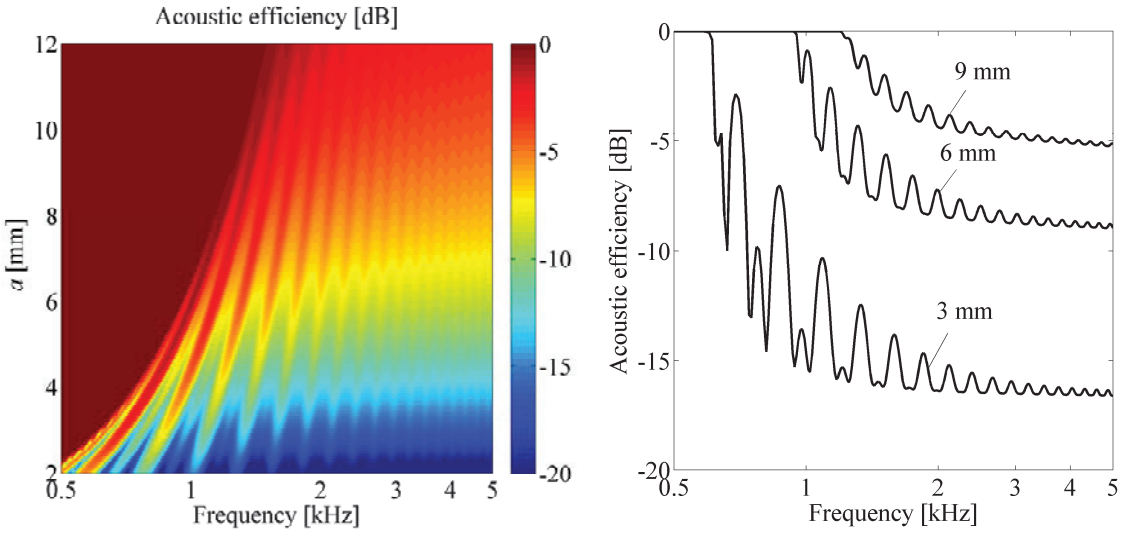

Figure 6 – Effect of the hole radius on the acoustic efficiency. (Left) Contour map and (Right) acoustic efficiency curves for several radiuses.

3.2.2 Influence of the spacing of the holes

Figs. 7 and 8 show the impact of the spacing of the holes on the directivity index and acoustic efficiency, respectively. The spacing of the holes was varied from 15 to 35 mm whereas all other parameters were held constant. The upper limit of analysis was chosen so as to avoid high order peaks (see Figure 8) occurring because of the resonance effect between adjacent holes (i.e., spacing of the holes that correspond to half-wavelength), resulting in high level side lobes in the polar response.

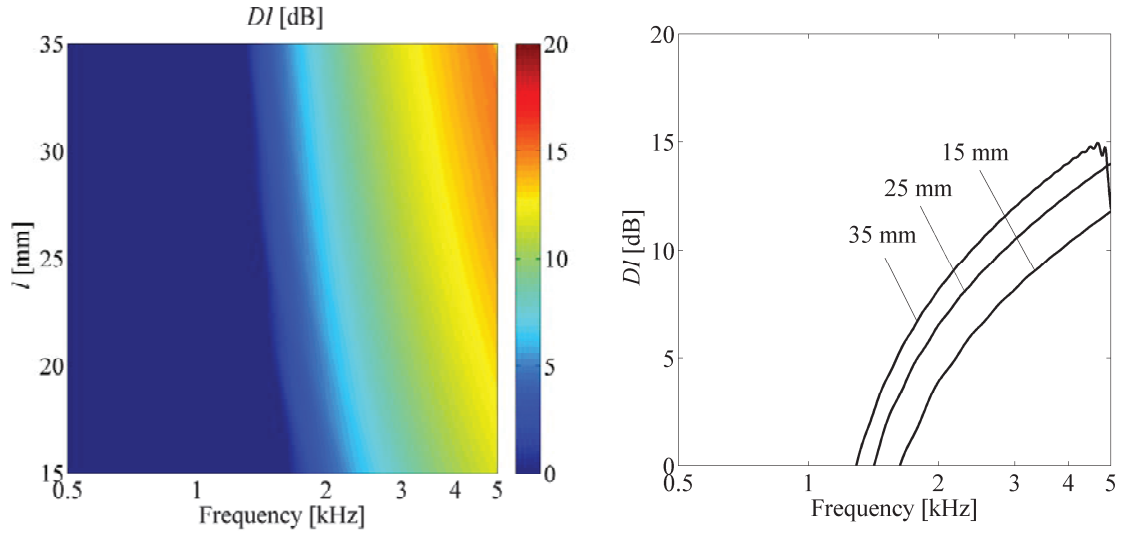

Figure 7 – Effect of the spacing of the holes on the directivity index. (Left) Contour map and (Right) directivity index curves for several spacings.

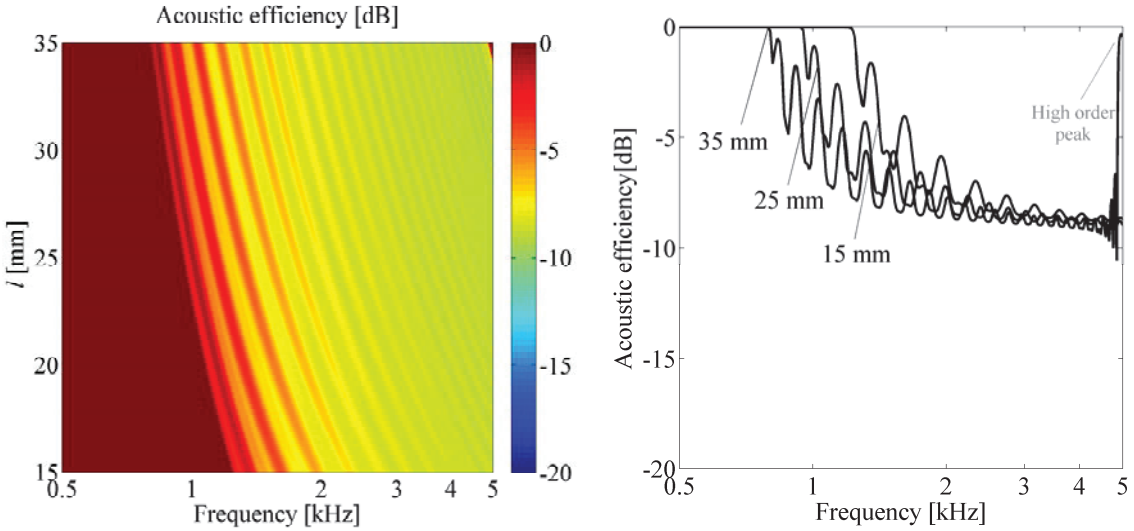

Figure 8 – Effect of the spacing of the holes on the acoustic efficiency. (Left) Contour map and (Right) acoustic efficiency curves for several spacings.

. In these figures, it becomes clear that the increasing spacing has the opposite effect to vary the radius of the holes since the directivity control improves while the acoustic efficiency diminishes. Anyway, spacing of the holes will not greatly impact the cut-off frequency despite its variation being several orders of magnitude higher than the hole size. Nevertheless, this effect is also linked to the increase of the array length and is difficult to estimate its contribution alone.

3.2.3 Summary

Figure 9 summarizes the effect of modifying the array geometrical parameters (hole size and spacing of the holes) on the full-band frequency averaged values of the directivity index and the acoustic efficiency. It is seen that, as expected, as the array becomes more directional the acoustic efficiency decreases, and vice versa. It reveals thus that the trends in both parameters are obviously opposed and confirms the previously mentioned trade-off therebetween.

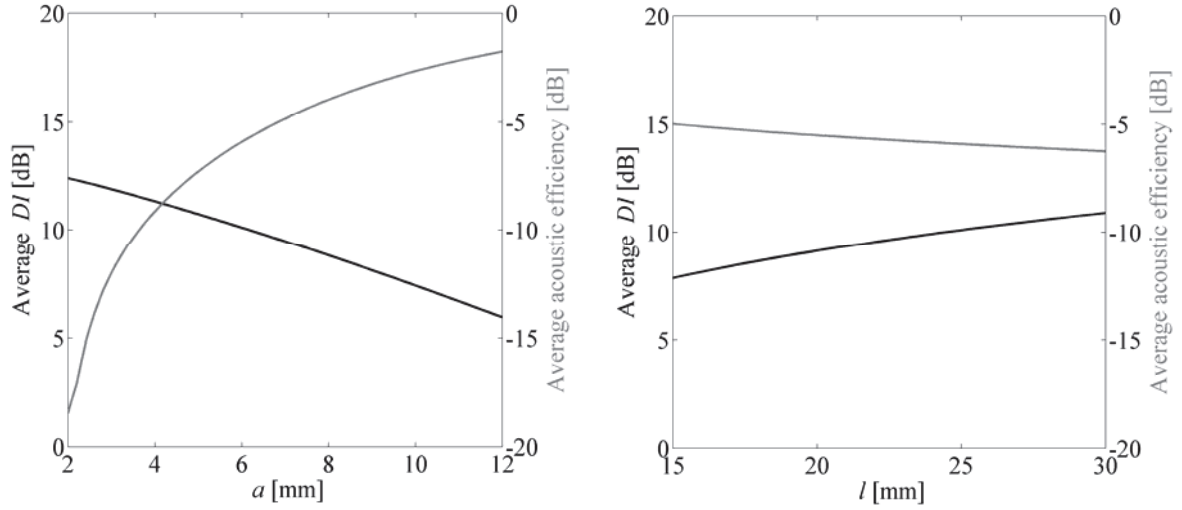

Figure 9 – Full-band frequency averaged values of the directivity index and the acoustic efficiency as a function of the hole radius (Left) and the spacing of the holes (Right).

3.3 Validation of the analytical model

To verify the correctness of the analytical approach, a comparison with the numerical model was performed. For this purpose, the reference array design is considered and the propagation constant calculated. Note that for the analytical prediction it is sufficient to consider one single hole section of the array instead of the whole array provided that the holes are periodically arranged. In Figure 10, results corresponding to the propagation constant obtained from Eq. (10) are compared with those provided by the numerical model (in which the expression of Z_h has been modified accordingly)

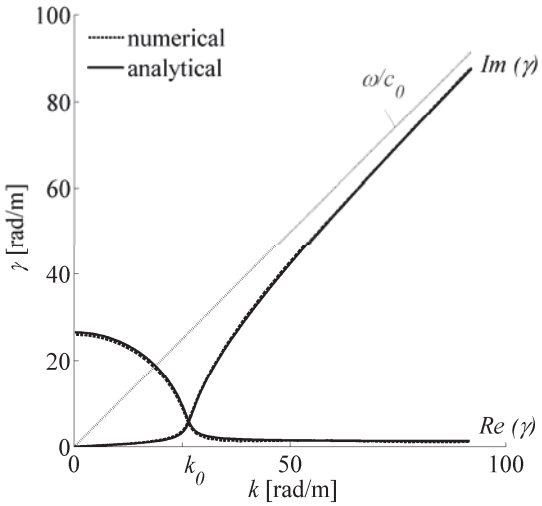

Figure 10 – Comparison of the propagation constant calculated using the numerical model and obtained using the proposed analytical model for the reference array design.

An excellent agreement is found is found for both approaches. For the reference design, the analytical model is able to predict correctly the sound propagation throughout the array. Also, these results demonstrate that for values of k greater than $k_0 = 2\pi f_0/c_0$, the phase shift approaches the wave number in air, which means that the wave attenuation between holes is negligible; whereas that for values of k smaller than k_0, the attenuation curve increases as the frequency lowers. In other words, at frequencies below f_0 the array behaves like an omnidirectional source due to the fact that only the first holes radiate sound effectively because of the high attenuation in the array system. This statement is

confirmed in the Sound Pressure Level results that were shown in Figure 4. It should be recalled that the analytical model is less complex than the numerical one and does not require the application of calculus, as it can be solved with linear algebra, with the advantage that a wide range of configurations can be examined with a very low time-consuming.

3.4 Remarks

The approaches whose results were presented above can be valid only under a series of conditions, so it is thus of great importance to tackle some of the limitations of these. The array description derived in both models states that the acoustic field in each hole is independent of the field in the neighboring holes. This assumption implies that the spacing of the holes is large enough and no interaction effect between holes must be considered, modified formulations being necessary otherwise. Hence, one has to be aware that this way of modeling is not strictly valid for closely separated holes configurations. On the other hand, care must also be taken regarding the effects of finite dimensions of the array for practical applications. Since both approaches assume the holes being baffled in an infinite screen, additional corrections must be carried out to account for the diffractive effects. Nonetheless, the models are able to capture most of the underlying physics related to this type of sound sources in a simple and straightforward manner without the need of more complex numerical methods.

4. CONCLUSIONS

This work was focused on the modeling of low-cost end-fire arrays to be used as AVAS in EVs. For this purpose, a numerical model of the array based on transmission line theory was computationally implemented and the acoustic performance of this system assessed. A parametric study was found very useful to investigate the influence of the array's geometrical parameters on the system response and in understanding the behaviour of the acoustic radiator. In this regard, assessment of the geometry effect on its directivity and acoustic efficiency is of great interest to the analysis and design of these sound sources. Additionally, the well-established equivalent circuit theory was used to propose an analytical model of the acoustic radiator, being validated against the numerical model with good agreement. The analytical approach turned out to be simpler than the former and served to study the sound wave propagation throughout the array. This research is of great importance in the context of the automotive industry since it provides a vehicle NVH analysis tool for the design of low-cost warning sound systems. These devices are intended to be a less expensive alternative to traditional ones along to allow greater directivity control (especially in low frequency). Even though further research is needed to assess the array's practical application, preliminary results are promising and encourage work on the development of low-cost end-fire arrays for their use in the automotive industry.

ACKNOWLEDGEMENTS

This work was partially funded by the COST Action - Transport and Urban Development - TU1105.

REFERENCES

1. Marbjerg G. Noise from electric vehicles - a literature survey. Compett, 2013.
2. Nordelöf A, Messagie M, Tillman A-M, Söderman MJ, Van Mierlo J. Environmental impacts of hybrid, plug-in hybrid, and battery electric vehicles - what can we learn from life cycle assessment? Int J Life Cycle Assess 2014; 19: 1866-1899.
3. European Environment Agency. Noise in Europe 2014. 2014.
4. European Environment Agency. Evaluating 15 years of transport and environmental policy integration - TERM 2015: Transport indicators tracking progress towards environmental targets in Europe. 2015.
5. NHTSA. Quieter cars and the safety of blind pedestrians: Phase I. 2010.
6. NHTSA. Minimum sound requirements for hybrid and electric vehicles - Draft environmental assessment. 2013.
7. ISO/FDIS 16254. Acoustics - Measurement of sound emitted by road vehicles of category M and N standstill and low speed operation - Engineering method (under development).
8. Misdariis N, Grunson A, Susini P. Detectability study of warning signals in urban background noises: A first step for designing the sound of electric vehicles. Proc 21st International Congress on Acoustics; 2-7 June 2013; Montreal, Canada 2013.
9. Sandberg U. Adding noise to quiet electric and hybrid vehicles: an electric issue. Acoust Aust. 2012; 40(3):211-220.

10. Goodes P, Bai YB, Meyer E. Investigation into the detection of a quiet vehicle by the blind community and the application of an external noise emitting system. SAE 2009 Noise and Vibration Conference and Exhibition.
11. Pedersen TH, Gadegaard T, Kjems K, Skov U. White paper on external warning sounds for electric cars-Recommendations and guidelines. Delta, 2011.
12. Cheer J, Birchall T, Clark P, Moran J, Elliott SJ, Fazi FM. Design and implementation of a directive electric car warning sound. Proc Institute of Acoustics; 2013; Saint Albans, Great Britain 2013.
13. Holland KR, Fahy FJ. A low-cost end-fire acoustic radiator. J Acoust Soc Am. 1991; 39 (7/8):540-550.
14. Konet H, Sato M, Schiller T, Christensen A, Tabata T, Kanuma T. Development of approaching Vehicle Sound for Pedestrians (VSP) for quiet electric vehicles. SAE Int J Engines 2011; 4(1): 1217:1224.
15. Kinsler LE, Frey AR, Coppens AB, Sanders JV. Fundamentals of acoustics. 4th ed.; Wiley; 1999.
16. Beranek LL, Mellow T. Acoustics: sound fields and transducers. 1st ed.; Academic Press; 2012.